

Optimization design of an Isolated DC/DC Converter Using Series Compensation on the Secondary Side

Satoshi Miyawaki

Student Member, IEEE
Nagaoka University of Technology
1603-1 Kamitomioka-cho Nagaoka
City
Niigata, Japan
miyawaki@stn.nagaokaut.ac.jp

Jun-ichi Itoh

Member, IEEE
Nagaoka University of Technology
1603-1 Kamitomioka-cho Nagaoka
City
Niigata, Japan
itoh@vos.nagaokaut.ac.jp

Kazuki Iwaya

Member, IEEE
TDK-LAMBDA, Ltd
2701 Tokawa Settaya Nagaoka City
Niigata, Japan
k.iwaya@jp.tdk-lambda.com

Abstract – This paper proposes a new circuit topology for a high efficiency isolated buck-boost DC/DC converter. The proposed converter consists of a high efficiency resonance half-bridge converter and a series converter. This proposed circuit regulates the output voltage by the series converter, which provides only the differential voltage between the input voltage and the output voltage. Therefore, the circuit achieves high efficiency when the input voltage is closed to the nominal voltage, since only the resonance converter will operate. The equivalent circuit of the proposed circuit is mentioned to clarify the circuit operation and circuit design. The experimental results confirmed that the proposed circuit, which converts 48-V input to 12-V output, achieves the maximum efficiency of 94.0% at the nominal input voltage region. Besides, the loss analysis is performed to optimize the circuit parameters.

Index Terms-- DC/DC converter, Isolated converter, Series voltage compensation, Current resonance

I. INTRODUCTION

Recently, high efficiency and high power density of power supplies are increasingly desired for telecom applications and microprocessor boards. In addition, these power converters have to supply larger output current with very low output voltage for the loads. In order to achieve high efficiency and high power density, the power system is divided into several converters, such as point-of-load converter, bus converters and front end converter. In this system, the power is distributed to each of the device by a DC voltage line [1-5].

The DC bus converter, which regulates the constant DC voltage for the output side, is required at the input point of each device because the DC bus voltage will fluctuate due to the bus impedance when the load condition had changed. The DC bus converter is also used to obtain different levels of DC voltage from the DC bus voltage. Therefore, high efficiency DC/DC converters are required for these bus converters.

Resonant type half-bridge converters, which use resonance between the leakage inductance of transformers and the DC capacitor, are one of the most effective circuit topologies to obtain high efficiency. However, it is difficult to regulate the output voltage in a wide range while there is a

fluctuation in the input voltage because the switching timing is constrained by the resonance period. Therefore, a resonant-type half-bridge converter is generally connected to a voltage control converter, such as a buck chopper [6-7]. As a result, the converter loss increases because all the power passes through two converters; the voltage control converter and the resonant converter.

This paper proposes a new topology for an isolated DC/DC converter using a series voltage compensation. The input voltage fluctuation is compensated by the auxiliary circuit that outputs only the fluctuation of the output voltage [8-11]. One of the advantages of the proposed circuit is that high efficiency can be achieved when the input voltage is closed to the nominal input voltage because the power of the auxiliary circuit becomes very small in comparison to the input power. Generally, the large fluctuations of the DC bus voltage are not generated for long periods, and as a result, the converter loss can be reduced.

Firstly, the approach used to obtain high efficiency with the proposed series compensation method is introduced in this paper. The circuit configuration and the control strategy are described accordingly. Secondly, the operation mode is analyzed using a simple equivalent circuit of the proposed circuit. The stability of the operation in the proposed circuit is clarified. In addition, the design strategy for optimization is clarified. Finally, some experimental results and loss analysis are given in order to demonstrate the advantages of the proposed converter.

II. CIRCUIT CONFIGURATIONS

A. Conventional Circuit

Fig. 1 shows a configuration of a conventional DC/DC converter. The conventional circuit consists of a resonant half-bridge converter and the voltage control converter, such as a buck boost chopper. The fluctuation of the input voltage is constantly controlled by the buck chopper. The output side is isolated by the resonant half-bridge converter to the input side. This system has two stages of the power flow from

input to output. The total efficiency of the conventional circuit η_c is obtained from (1); using both the resonant converter efficiency η_1 and the buck chopper efficiency η_2 .

$$\eta_c = \eta_1 \eta_2 \quad (1)$$

All the power passes through both converters despite the relation with the input voltages; therefore, the converter efficiency is decreased.

B. Proposed Circuit

Fig. 2 shows the configuration of the proposed converter using series connection on secondary side. In the proposed circuit, this system consists of two power converters; main circuit and auxiliary circuit, which are connected in series to the output side using a transformer.

The main circuit is the resonant type half-bridge converter with isolation transformer. Zero current switching (ZCS) is implemented by the resonance circuit between the leakage inductance of the transformer and the resonance capacitor in the DC part, in order to achieve high efficiency. The switching frequency of the main circuit is constrained by the resonance frequency f_0 .

The switching frequency of the main circuit is constrained by the resonance frequency f_0 . From the equivalent circuit of the transformer shown in Fig. 2(a), the resonant inductance of the proposed circuit L is obtained from (2), using the leakage inductance l_{xx} , mutual inductance M_{xx} and the number of wire turns N_{xx} .

$$L = l_{11} + \frac{M_1(l_{12} + L_{T2})}{M_1 + (l_{12} + L_{T2})} \quad (2)$$

$$\text{where, } L_{T2} = \left(\frac{N_{11}}{N_{12}} \right)^2 \left(\frac{N_{22}}{N_{21}} \right) \left(l_{21} + \frac{l_{22} M_2}{l_{22} + M_2} \right)$$

The resonance frequency of the proposed circuit f_0 is obtained by (3).

$$f_0 = \frac{1}{2\pi\sqrt{LC}} \quad (3)$$

On the other hand, the auxiliary circuit is the full-bridge converter uses for regulating the output voltage. The output voltage of the auxiliary circuit is added to the output of the main circuit by the transformer. That is, the auxiliary circuit compensates only the fluctuation voltage, against the output voltage commands.

The proposed system consists of two power converters, which are connected in series to the output side. The reason for high efficiency in the proposed circuit is as follows. The power P_{out} is obtained by adding the auxiliary converter power P_3 to the directly power P_0 , as shown by Fig. 2(b). The total converter efficiency of the proposed circuit η_p is obtained by (4), using the auxiliary circuit efficiency η_3 and the power ratio $k=P_3/P_0$.

$$\eta_p = \eta_1 \frac{1+k\eta_3}{1+k} \quad (4)$$

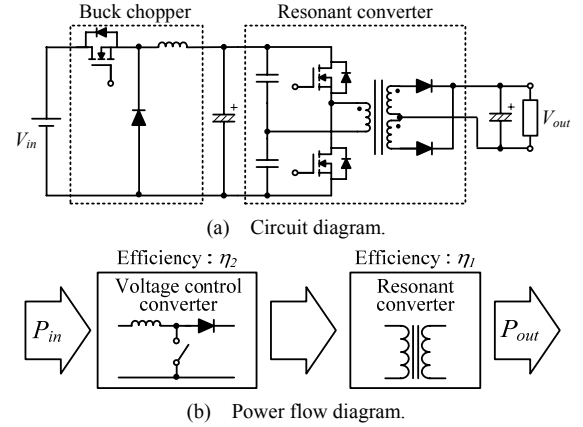


Fig. 1. Conventional circuit using a buck chopper and a resonant converter.

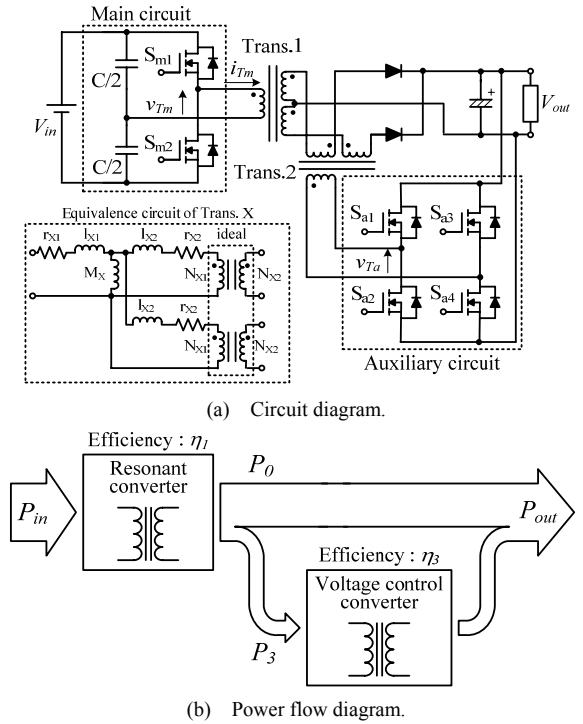


Fig. 2. Proposed circuit using series connection on secondary side.

It should be noted that the voltage rating of the switching device in the auxiliary converter is lower than the main circuit since the output voltage is lower than the input voltage. That is, the conduction loss of the auxiliary circuit can be decreased.

III. CONTROL STRATEGY

In the proposed circuit, the main circuit is controlled under an optimum condition as the resonant converter. In order to obtain the maximum efficiency, the resonant converter operates at 50% duty cycle based on the resonance frequency f_0 . Therefore, the main circuit can achieve zero current

switching (ZCS) at any time.

Fig. 3 shows the operation mode and the waveforms in the primary side of the transformer in the boost mode. The switching timing of the auxiliary circuit is synchronous with the main circuit. The auxiliary circuit can output three different voltage levels; $+V_{out}$, $-V_{out}$, and zero voltage. In the boost mode; i.e. when the input voltage is decreased, the auxiliary circuit outputs positive phase voltage to the output voltage of the main circuit without preventing the resonance operation in the main circuit. Similarly, in the buck mode; i.e. when the input voltage is increased; the auxiliary circuit outputs negative phase voltage to the output voltage of the main circuit.

The output voltage is controlled by changing the pulse width D of the auxiliary circuit. If the voltage drop from the leakage inductance and winding resistance are negligible, the pulse width of the auxiliary circuit D is obtained by (6), using the switching (resonance) cycle T and the output voltage command V_{out}^* .

$$D = \frac{T}{2} \cdot \frac{N_{21}}{N_{22}} \cdot \left(\frac{V_{out}^*}{V_{out}} - \frac{N_{12}}{2N_{11}} \cdot \frac{V_{in}}{V_{out}} \right) \quad (6)$$

Fig. 4 shows the control block diagram of the proposed circuit. The duty cycle of the main circuit is set to 50%. In the auxiliary circuit, the output pulse width D is calculated by an automatic voltage regulator (AVR) according to output voltage command. The phase shift gain is then calculated by D . The phase shift is used to decrease the switching loss in the auxiliary circuit, because the phase of the output voltage in the auxiliary circuit can be adjustable to the phase of the output voltage in the main circuit. According to the relation between the output and input voltages, the mode selector determines the operation mode. It should be note that the proposed converter has the reference voltage mode, which means that the auxiliary circuit stops when the input voltage is almost the same as the nominal input voltage, in addition to the buck and boost mode operation.

IV. OPERATIONAL MODE ANALYSIS

A. Simple Equivalent Circuit

The proposed circuit is clarified in order to understand the stability of operation and the operational mode is analyzed using a simple equivalent circuit. Fig. 5 shows the equivalent circuit of the proposed circuit under the boost operation. In the AC signal analysis, the switching operation of the main circuit and the rectifier part at the output side is expressed as a square wave power source, which has the amplitude of the input and output voltage at the frequency of the switching frequency respectively. The capacitors of the half-bridge converter can be represented as one resonance capacitor with ideal transformers. Moreover, the full-bridge converter in the auxiliary circuit is represented as three different voltage levels; $+V_{out}$, $-V_{out}$, and zero voltage. Note that the excitation inductance of the transformer is disregarded in the analysis

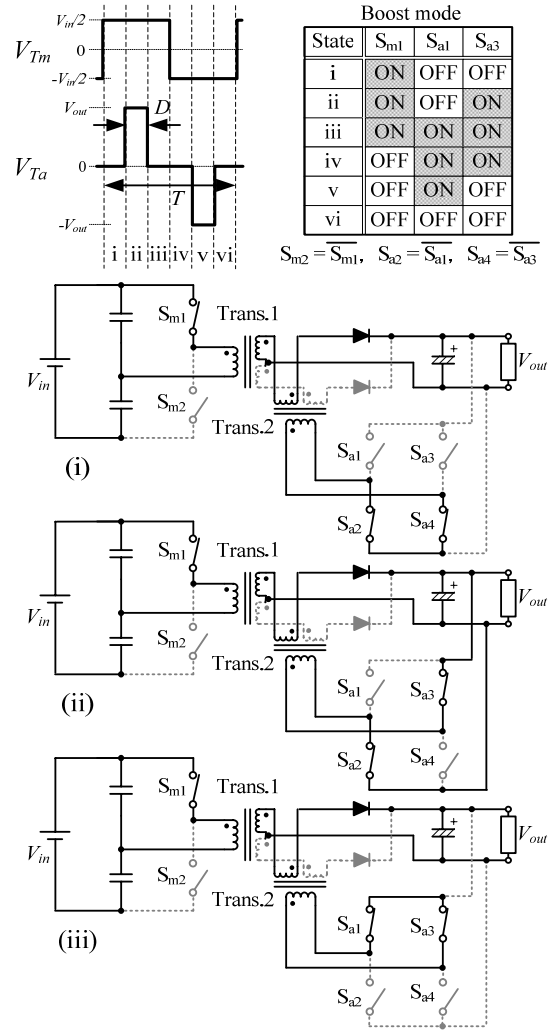


Fig. 3. Corresponding of the switching pattern and operation mode.

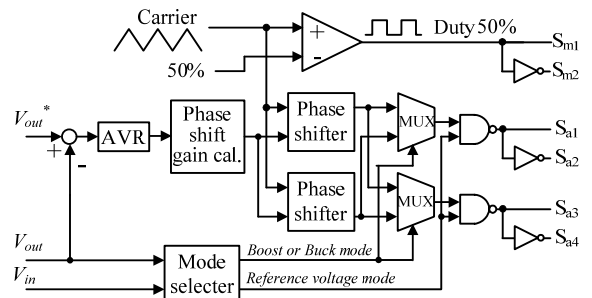


Fig. 4. Control block diagram of the proposed circuit.

because it is much larger than the leakage inductance. The resonance frequency is dominated by the leakage inductance.

B. Derivation of the circuit equation

Fig. 6(a) and (b) show the simplified equivalent circuit which is separated into the main circuit side and auxiliary circuit side, according to the superposition principle. The

separation of the equivalent circuit is achieved by focusing on the transformer input current i_{Tm} of the main circuit. The equivalent circuit is obtained from the perspective of the main circuit, when the input of the auxiliary circuit is short-circuited. Similarly, the equivalent circuit is obtained from the perspective of the auxiliary circuit, when the input of the main circuit is short-circuited; i_{Tm} is obtained by (7).

$$i_{Tm} = i_{Tm_m} + i_{Tm_a} \quad (7)$$

where i_{Tm_m} is the input current on the main circuit side as shown in Fig. 6(a) and i_{Tm_a} is the input current on the auxiliary circuit side as shown in Fig. 6(b). Consequently, the equation of the entire circuit can be obtained by deriving each equation from each of the circuit equation in Fig. 6. The input current i_{Tm_m} and i_{Tm_a} are obtained from (8) and (9).

$$i_{Tm_m} = e^{-\frac{1}{\tau}t} \left[\begin{aligned} & \frac{1}{2} \cdot \frac{V_{in}}{\omega L} \sin(\omega t) - \frac{\alpha V_{out}}{\omega L} \sin(\omega t) \\ & + i_{m(k)} \left\{ \cos(\omega t) - \frac{1}{2Q} \sin(\omega t) \right\} - q_{m(k)} \omega \left(1 + \frac{1}{4Q^2} \right) \sin(\omega t) \end{aligned} \right] \quad (8)$$

$$i_{Tm_a} = e^{-\frac{1}{\tau}t} \left[\begin{aligned} & \frac{\alpha}{\beta} \cdot \frac{V_{out}}{\omega L} \sin(\omega t) - \frac{\alpha \Delta V_{out}}{\omega L} \sin(\omega t) \\ & + i_{a(k)} \left\{ \cos(\omega t) - \frac{1}{2Q} \sin(\omega t) \right\} - q_{a(k)} \omega \left(1 + \frac{1}{4Q^2} \right) \sin(\omega t) \end{aligned} \right] \quad (9)$$

$$\text{where, } \tau = \frac{2L}{R}, \quad \omega = \sqrt{\frac{1}{LC} - \left(\frac{1}{\tau}\right)^2}, \quad Q = \frac{\omega L}{R}$$

$$R = R_1 + \left(\frac{\alpha}{\beta}\right)^2 R_2, \quad L = L_1 + \left(\frac{\alpha}{\beta}\right)^2 L_2$$

$i_{m(k)}$ and $i_{a(k)}$ are the initial currents of the leakage inductions, and $q_{m(k)}$ and $q_{a(k)}$ are the initial charges of resonance capacitor for the main and auxiliary sides, respectively. The optimization design of the proposed circuit can be obtained from this equation.

V. DESIGN OPTIMIZATION METHOD

A. Outline of the circuit design

Fig. 7 shows the design flowchart for the proposed circuit. Optimization of the design is achieved by following the design flow. Firstly, the five circuit design specifications are determined by applications, which consist of the volume of the circuit, the minimum power of the stable operation area P_{min} , the fluctuation range of the input voltage V_{fluc} , the input and output voltage V_{in} , V_{out} , and the rated power P_{max} . The resonance frequency is determined by the switching frequency. The resonance impedance is then designed based on the specifications. Specifically, the minimum value of the resonance inductance L is limited by the minimum power of the stable operation area P_{min} . After L is determined, resonant

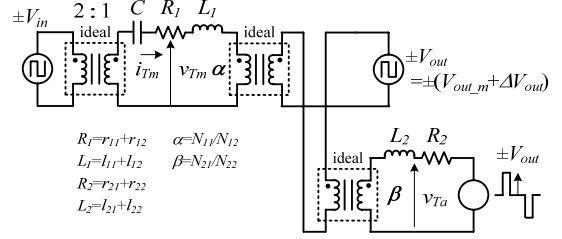
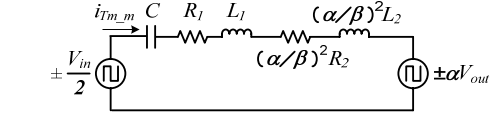
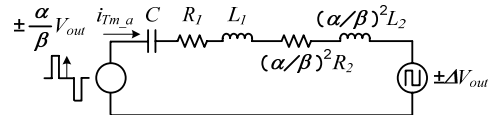


Fig. 5. Simple equivalent circuit



(a) Only main circuit.



(b) Only auxiliary circuit.

Fig. 6. Separation of circuit by superposition principle.

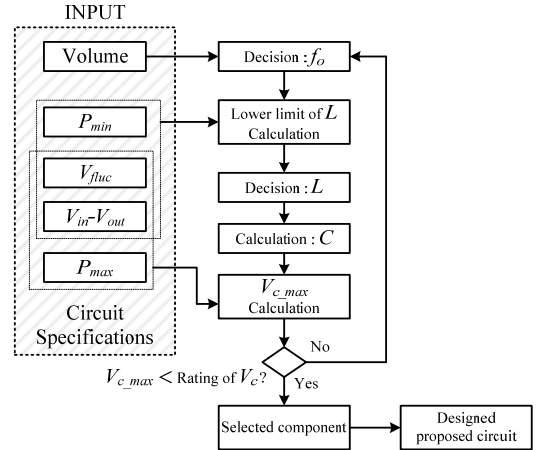


Fig. 7. Optimization design procedure flowchart.

capacitor C can be obtained by (3) according to the resonance frequency. Note that the resonance impedance needs to be adjusted accordingly so that the maximum voltage of C is not larger than the minimum input voltage.

B. Determination of the resonant impedance

In order to control the output voltage, a stable operation is required. The discontinuance mode of the resonance current causes instability in the light load area. The boundary condition indicates the edge state between the continuous and discontinuous current. The boundary condition for the stable operation depends only on the operation of the auxiliary circuit in Fig. 6(b). In this state, the peak value of the transformer current increases significantly compared to the continuous mode because the same output power is obtained

as the boundary condition using a narrow current pass period. The instability problem also encountered for discontinuous current mode of a boost reactor in a chopper circuit. Therefore, the continuous mode has to be maintained until the minimum power P_{min} is outputted. The lower limit in the light load in where the continuous mode is maintained depends on the resonance impedance.

Fig. 8 shows the resonant current waveforms for the separate auxiliary circuit shown in Fig. 6(b). At the boundary condition in section (i), the current value $i_{Tm,a}$ until t_1 is zero because the boundary condition indicates the edge state between the continuous and discontinuous current. Next, $i_{Tm,a}$ in section (ii) can be obtained from (10) using a linear approximation according to the inductance L and output voltage. Note that the capacitor voltage is equaled to the average value of the output voltage for one switching period in the auxiliary circuit ΔV_{out} .

$$i_{Tm,a(ii)} = \frac{\alpha}{\beta} \cdot \frac{V_{out}}{L} D \quad (10)$$

Input current on the auxiliary circuit side $i_{Tm,a}$ becomes the maximum at t_2 , and decreases in section (iii). The output voltage period (output pulse width D in the auxiliary circuit) is limited according to (11).

$$2D_0 > \frac{T}{2} - D \quad (11)$$

where D_0 is the zero voltage period of the auxiliary circuit for a half cycle.

When, the linear approximation is used, the current waveform is approximated to be a triangular shape. Therefore, the mean current value I_0 for the half cycle is obtained by (12).

$$I_0 = \frac{2}{T} \left\{ \frac{1}{2} \cdot \frac{\alpha}{\beta} \cdot \frac{V_{out}}{L} D (D + D_0) \right\} \quad (12)$$

On the other hand, the mean current value I_0 is obtained from the output power with (13), using the load resistance R_L and the average value of the output voltage in the auxiliary circuit ΔV_{out} .

$$I_0 = \frac{\Delta V_{out}}{\alpha R_L} \quad (13)$$

Thus, the range of L for stable operation is obtained by (14), using (11) to (13).

$$L \geq \frac{\alpha^2 V_{out}^3 D}{4\beta \cdot \Delta V_{out} \cdot P_{min}} \left(1 + \frac{D}{T/2} \right) \quad (14)$$

where, $P_{min} = \frac{V_{out}^2}{R_L}$

Consequently, the minimum value of L is limited by the output pulse width D and the load condition. That is, the minimum reactor is increased according to the minimum power P_{min} in the specification.

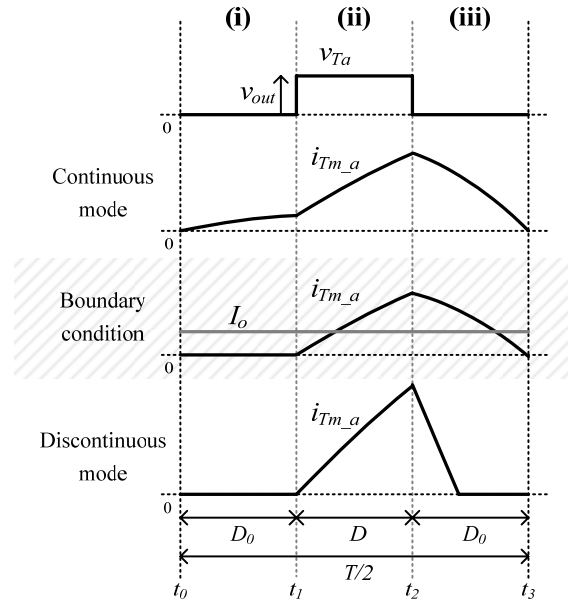


Fig. 8. Resonant current waveforms only on separating auxiliary circuit in Fig. 6(b).

TABLE I
CIRCUIT SPECIFICATIONS

$V_{in} - V_{out}$	48V - 12V
V_{fluc}	12V ($\pm 25\%$)
P_{min}	75W
P_{max}	200W
f_o	220kHz

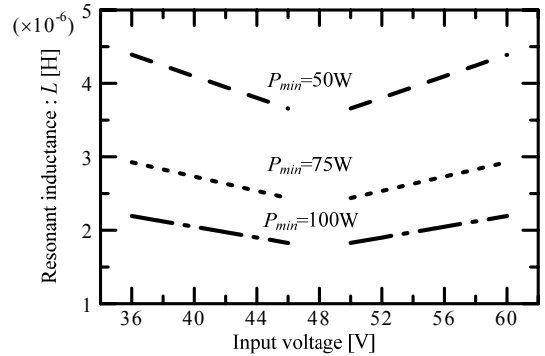


Fig. 9. Calculation results of the Lower limit of resonant inductance.

C. Design Example

Table 1 shows the specifications for the circuit. When the reference voltage mode, the proposed circuit converts 48 V input to 12 V output. The input voltage 48 V is fluctuating $\pm 25\%$. The optimization value at 220-kHz resonant frequency is used. From the relations between the input and output voltage, transformer turns ratio of the main circuit is $N_{11}:N_{12}=2:1$. From the V_{fluc} , transformer turns ratio of the

auxiliary circuit is $N_{21}:N_{22}=2:1$.

Fig. 9 shows the value of the minimum resonance inductance is obtained by (14) using the specifications given in Table 1. When $P_{out} = 75$ W, approximately $2.8 \mu\text{H}$ is necessary for the resonance inductance. The inductance is inserted in series to the primary side of the transformer in the main circuit, because the leakage inductance of the main transformer is insufficient. Moreover, C is determined by (3) to be $0.20 \mu\text{F}$.

The maximum value of the resonance current I_{max} is then obtained from (15), using the maximum power P_{max} .

$$I_{max} = 2 \frac{P_{max}}{V_{in}} \cdot \frac{\pi}{2} = 13A \quad (15)$$

Therefore, the maximum value of the resonant capacitor voltage V_{c_max} can be obtained from (16).

$$V_{c_max} = \frac{I_{max}}{\omega C} = 47V \quad (16)$$

V_{c_max} is lower than the input voltage. Consequently, each element in the proposed circuit is selected according to the specifications given in Table 1.

VI. EXPERIMENTAL RESULT

At first, experimental results of the main circuit are presented in order to confirm the high efficiency can be achieved in the main circuit. Then, experimental results of the proposed circuit are presented at the second.

A. Experimental results of the main circuit

Fig. 10 shows the load characteristics of the main circuit (input voltage: 48V). The turn ratio of the transformer in the main circuit was 2:1. Therefore, the output voltage becomes 12V when the input voltage of the main circuit is 48V. However, the control method is an open-loop control, that is, the duty cycle is set to 50%. As a result, the maximum efficiency of 94.0% is obtained at load of 60 W, as shown in Fig. 10. It is confirmed that the high efficiency is achieved in the main circuit. It should be noted that the synchronous rectification using MOSFET is applied to the secondary side in order to reduce the conduction losses of the rectifier.

B. Experimental results of the proposed circuit

Fig. 11 presents the efficiency of the proposed converter at a constant load (cf., Table 1) when the input voltage has fluctuation of $\pm 25\%$. In order to confirm the validity of the concept, the proposed converter was tested. The maximum efficiency of 94.0% is obtained, as shown in Fig. 11, when the input voltage is much closed to the nominal input voltage. The reason for low efficiency in the boost mode compared to the buck mode is that the current in the boost mode is increased by the circulation current between the auxiliary circuit and the rectifier. Consequently, the conduction loss is increased by the circulating current.

Fig. 12 and Fig. 13 show the input current of the

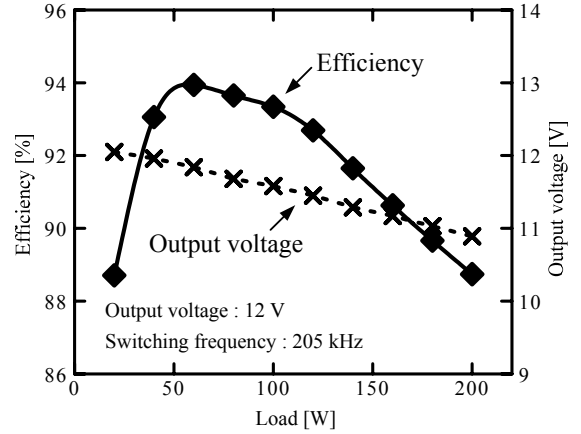


Fig. 10. Load characteristics of the main circuit.

TABLE II
EXPERIMENTAL PARAMETERS

Nominal input voltage	48 V	Wire turns Trans. 1	2 : 1
Input voltage fluctuation range	12 V ($\pm 25\%$)	Wire turns Trans. 2	2 : 1
Output voltage	12 V	Resonance Capacitance (C)	0.2 μF
Output power	60,100W	Resonance Inductance (L)	2.4 μH
Switching frequency	205 kHz		

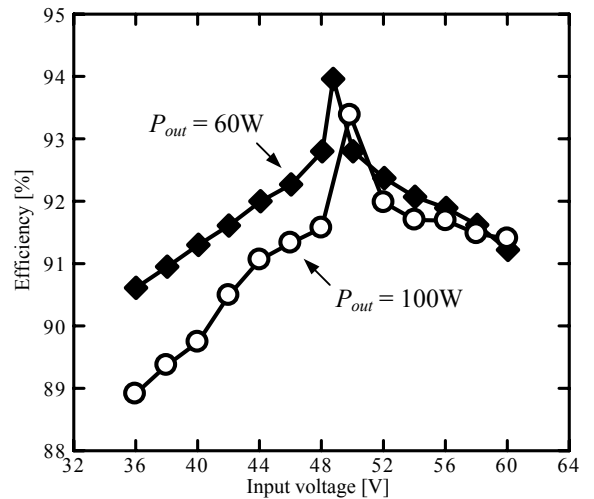


Fig. 11. Calculation results of the Lower limit of resonant inductance.

transformer and the terminal voltage of Sm2. In these modes, reference mode, boost and buck mode accordingly, the half-bridge converter maintain at zero current switching. A switching frequency of approximately 220 kHz was confirmed.

Fig. 14 shows the loss analysis of the proposed converter based on the simulated and experimental results. In order to

clarify the power loss of the proposed circuit, the loss measurement and analysis for each of the part have been examined. When the input voltage is very close to the nominal input voltage, the maximum efficiency of the proposed circuit is obtained. The auxiliary FET loss increases in both boost and buck modes, and the loss in the main transformer and main FET are predominant. Therefore, in order to obtain higher efficiency, the selection of FETs in the auxiliary circuit is important. The low on-state resistance device should be chosen because the voltage rating of the FET can be reduced in comparison with the main circuit. Besides, the parameters design of the transformer based on the equivalent circuit analysis are required.

VII. CONCLUSIONS

A series type isolated DC/DC converter consisting of a resonant-type half-bridge converter and an auxiliary converter has been proposed. The concept for the series compensation, which obtains the output voltage by adding or subtracting the auxiliary converter voltage to the half-bridge converter voltage, is proposed. The operation mode is analyzed using a simple equivalent circuit of the proposed circuit. Then, the stability of the operation for the proposed circuit is clarified. In addition, design optimization in the resonant impedance was clarified by using a design procedure flowchart.

The experimental results confirmed the maximum efficiency of 94.0% is obtained when the input voltage was closed to the nominal input voltage. It was confirmed that the voltage control can be regulated while maintaining high efficiency. From the loss analysis, the auxiliary FET loss increases in both the boost and buck modes, and the loss in the main transformer and main FET are predominant.

In future work, the circuit topology will be optimized to reduce the switch count in the auxiliary circuit.

REFERENCES

- [1] J.Biela, U.Badstuebner, J.W.Kolar, "Impact of Power Density Maximization on Efficiency of DC-DC Converter Systems", *IEEE Transaction on Power Electronics*, Vol.24, No.1, pp288-300, 2009.
- [2] Ming Xu, F.C.Lee, "General concepts for high-efficiency high-frequency 48 V DC/DC converter", *PESC '03. 2003 IEEE 34th Annual Volume 1*, pp 156-162, 2003.
- [3] P.Alou, J.A.Cobos, J.Uceda, M.Rascon, E. de la Cruz, "Design of a low output voltage DC/DC converter for telecom application with a new scheme for self-driven synchronous rectification", *APEC '99, Vol.2*, pp 866-872, 1999.
- [4] H.Mao, S.Deng, J.Abu-Qahouq, I.Batarseh, "Active-Clamp Snubbers for Isolated Half-Bridge DC-DC Converters", *IEEE Transaction on Power Electronics*, Vol.20, No.6, pp1294-1302, 2005.
- [5] K.Fathy, K.Morimoto, T.Do, H.Ogiwara, H.W.Lee, M.Nakaoka, "A Diveded Voltage Half-Bridge High Frequency Soft-Switching PWM DC-DC Converter with High and Low Side DC Rail Active Edge Resonant Snubbers", *IPEMC 2006, vol. 2*, pp. 1-5, 2006.
- [6] M.Takagi, K.Shimizu, T.Zaitus, "Ultra High Efficiency of 95% for DC/DC Converter - Considering Theoretical Limitation of Efficiency", *IEEE APEC 2002, vol. 2*, pp. 735-741, 2002.

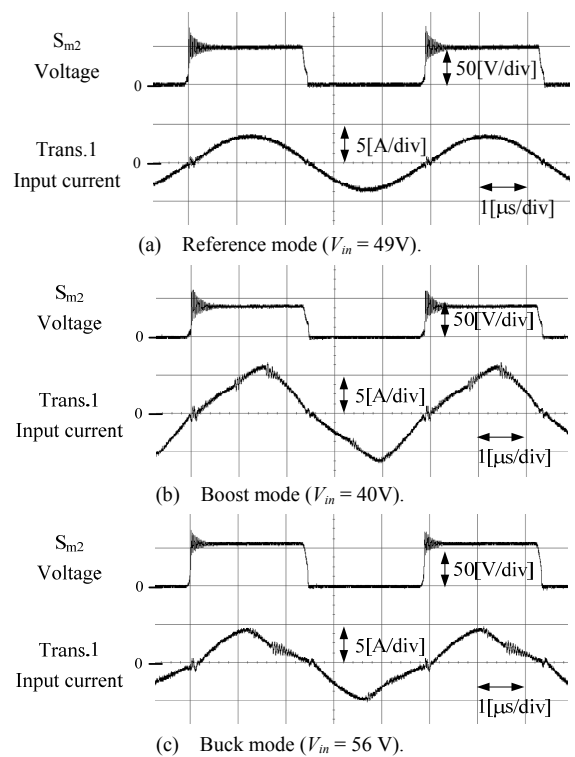


Fig. 12. Input current of the transformers and the terminal voltage of S_{m2} (Load: 60 W)

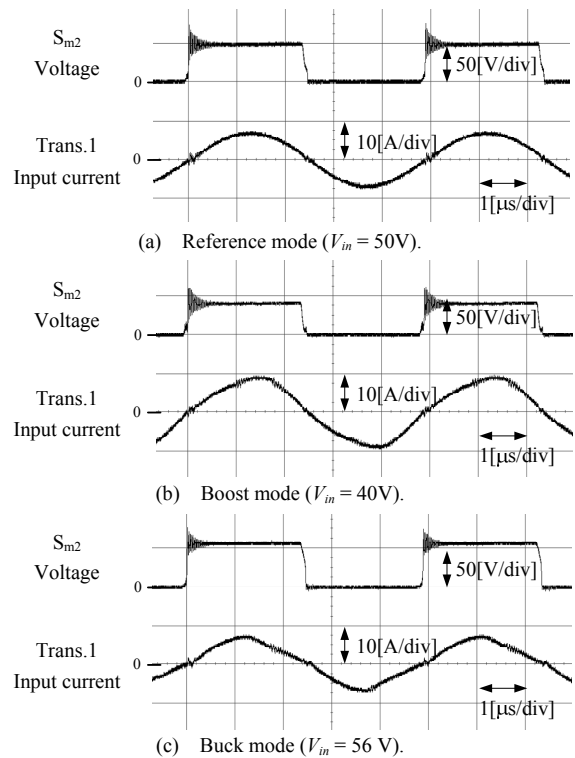


Fig. 13. Input current of the transformers and the terminal voltage of S_{m2} (Load: 100 W)

- [7] P.Alou, J.Oliver, J.A.Cobos, O.Garcia, J.Uceda, "Buck+half bridge (d=50%) topology applied to very low voltage power converters", *APEC 2001, Sixteenth Annual IEEE Volume 2*, pp 715-721, 2001.
- [8] G.Guidi, T.M.Undeland, Y.Hori, "An Interface Converter with Reduced VA Ratings for Battery-Supercapacitor Mixed Systems", *IEEE PCC 2007*, pp 936-941, 2007.
- [9] B.Min, J.Lee, J.Kim, T.Kim, D.Yoo, E.Song, "A New Topology with High Efficiency throughout All Load Range for Photovoltaic PCS", *IEEE Transaction on Industrial Electronics, Vol.56, No.11*, pp4427-4435, 2009..
- [10] J.Itoh, T.Fujii, "A new approach for high efficiency buck-boost DC/DC converters using series compensation", *PESC 2008.IEEE*, pp 2109-2114, 2008.
- [11] S.Miyawaki, J.Itoh, K.Iwaya, "High Efficiency Isolated DC/DC Converter Using series Voltage Compensation", *PCIM Europe 2009 Conference*, pp66-71, 2009.

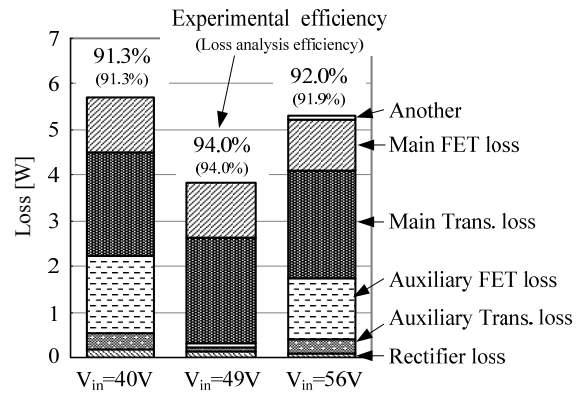


Fig. 14. Loss analysis at 60 W load.